© 2018. Published by The Company of Biologists Ltd | Journal of Cell Science (2018) 131, jcs219311. doi:10.1242/jcs.219311

SHORT REPORT

Biphasic recruitment of TRF2 to DNA damage sites promotes non-sister chromatid homologous recombination repair

Xiangduo Kong[1], Gladys Mae Saquilabon Cruz[2], Sally Loyal Trinh[1], Xu-Dong Zhu[3], Michael W. Berns[2,4,5,*] and Kyoko Yokomori[1,*]

ABSTRACT

TRF2 (TERF2) binds to telomeric repeats and is critical for telomere integrity. Evidence suggests that it also localizes to non-telomeric DNA damage sites. However, this recruitment appears to be precarious and functionally controversial. We find that TRF2 recruitment to damage sites occurs by a two-step mechanism: the initial rapid recruitment (phase I), and stable and prolonged association with damage sites (phase II). Phase I is poly(ADP-ribose) polymerase (PARP)-dependent and requires the N-terminal basic domain. The phase II recruitment requires the C-terminal MYB/SANT domain and the iDDR region in the hinge domain, which is mediated by the MRE11 complex and is stimulated by TERT. PARP-dependent recruitment of intrinsically disordered proteins contributes to transient displacement of TRF2 that separates two phases. TRF2 binds to I-PpoI-induced DNA double-strand break sites, which is enhanced by the presence of complex damage and is dependent on PARP and the MRE11 complex. TRF2 depletion affects non-sister chromatid homologous recombination repair, but not homologous recombination between sister chromatids or non-homologous end-joining pathways. Our results demonstrate a unique recruitment mechanism and function of TRF2 at non-telomeric DNA damage sites.

KEY WORDS: TRF2, TERF2, PARP1, DNA damage, Homologous recombination repair, MRE11 complex, Laser microirradiation

INTRODUCTION

TRF2 (also known as TERF2) is an integral component of the telomere shelterin complex that protects telomere integrity (Bilaud et al., 1997; Feuerhahn et al., 2015; Okamoto et al., 2013; van Steensel et al., 1998). TRF2 recognizes the telomere repeat sequence directly through its C-terminal MYB/SANT domain, and protects telomeres by both promoting T-loop formation and inhibiting the DNA damage checkpoint kinase, ATM (de Lange, 2002; Griffith et al., 1999; Karlseder et al., 2004; van Steensel et al., 1998). TRF2 has also been shown to be recruited to non-telomeric DNA damage sites and promote DNA double-strand break (DSB) repair, though its exact role in the process remains controversial. Recruitment of TRF2 has been observed at high-irradiance laser-induced DNA lesions, but not at damage sites induced by low-irradiance ultraviolet radiation or ionizing radiation, despite the presence of DSBs in both cases (Bradshaw et al., 2005; Huda et al., 2012; Williams et al., 2007). TRF2 has also been linked to homologous recombination (HR) repair (Mao et al., 2007), but its phosphorylation by ATM appears to be important for fast repair [suggested to be non-homologous end-joining (NHEJ)] (Huda et al., 2009). Thus, TRF2 recruitment and function at non-telomeric DNA damage sites remain enigmatic.

PARP1 is a DNA nick sensor activated rapidly and transiently in response to DNA damage (for reviews see Ball and Yokomori, 2011; Beck et al., 2014; Daniels et al., 2015; Kalisch et al., 2012). There are multiple PARP family members, but PARP1 plays a major role in poly(ADP-ribose) (PAR) response at damage sites (Cruz et al., 2015; Kong et al., 2011). Activated PARP1 uses NAD^+ as a substrate to ADP-ribosylate multiple target proteins, including itself. Although PARP1 was initially thought to specifically facilitate base excision repair and/or single-strand break repair, recent studies have revealed its role in multiple DNA repair pathways, including DSB repair (Beck et al., 2014). Furthermore, PAR modification at DNA damage sites is critical for the recruitment of chromatin modifying enzymes that promote DNA repair (Ahel et al., 2009; Ayrapetov et al., 2014; Ball and Yokomori, 2011; Chou et al., 2010; Gottschalk et al., 2009; Izhar et al., 2015; Khoury-Haddad et al., 2014; Larsen et al., 2010; Polo et al., 2010; Smeenk et al., 2010; Sun et al., 2009). Thus, PARP1 is not only a sensor of DNA damage, but also a regulator of damage site chromatin environment and multiple DNA repair pathways in higher eukaryotes.

RESULTS AND DISCUSSION

TRF2 recruitment to damage sites is determined by the degree of PARP activation

Previously, we found that TRF2 is rapidly recruited to higher input-power laser damage sites that contained complex DNA damage in a PARP-dependent manner (Cruz et al., 2015). In contrast, lower input-power laser irradiation that induced relatively simple strand-breaks and no significant PAR response failed to recruit TRF2 (for laser power measurements, see Materials and Methods). Importantly, stimulation of PARylation at lower input-power laser damage sites by a PARG inhibitor promotes TRF2 recruitment in HeLa cells (Fig. 1A). Therefore, the level of PARP activation, rather than the nature of damage per se, is the deciding factor for TRF2 recruitment to non-telomeric DNA damage sites.

Biphasic recruitment of TRF2 to damage sites

We and others have observed rapid and transient TRF2 recruitment to damage sites within the first 5 min post-irradiation (p.i.) (Bradshaw et al., 2005; Cruz et al., 2015) (Fig. 1). Upon

[1]Department of Biological Chemistry, School of Medicine, University of California, Irvine, CA 92697-1700, USA. [2]Beckman Laser Institute and Medical Clinic, University of California, Irvine, 1002 Health Sciences Road East, Irvine, CA 92612, USA. [3]Department of Biology, McMaster University, Hamilton, Ontario L8S 4K1, Canada. [4]Department of Developmental and Cell Biology, School of Biological Sciences, University of California, Irvine, CA 92617, USA. [5]Department of Biomedical Engineering and Surgery, University of California, Irvine, CA 92617, USA.

*Authors for correspondence (mwberns@uci.edu; kyokomor@uci.edu)

K.Y., 0000-0002-2785-4589

Received 20 April 2018; Accepted 30 October 2018

Journal of Cell Science (2018) 131, jcs219311. doi:10.1242/jcs.219311

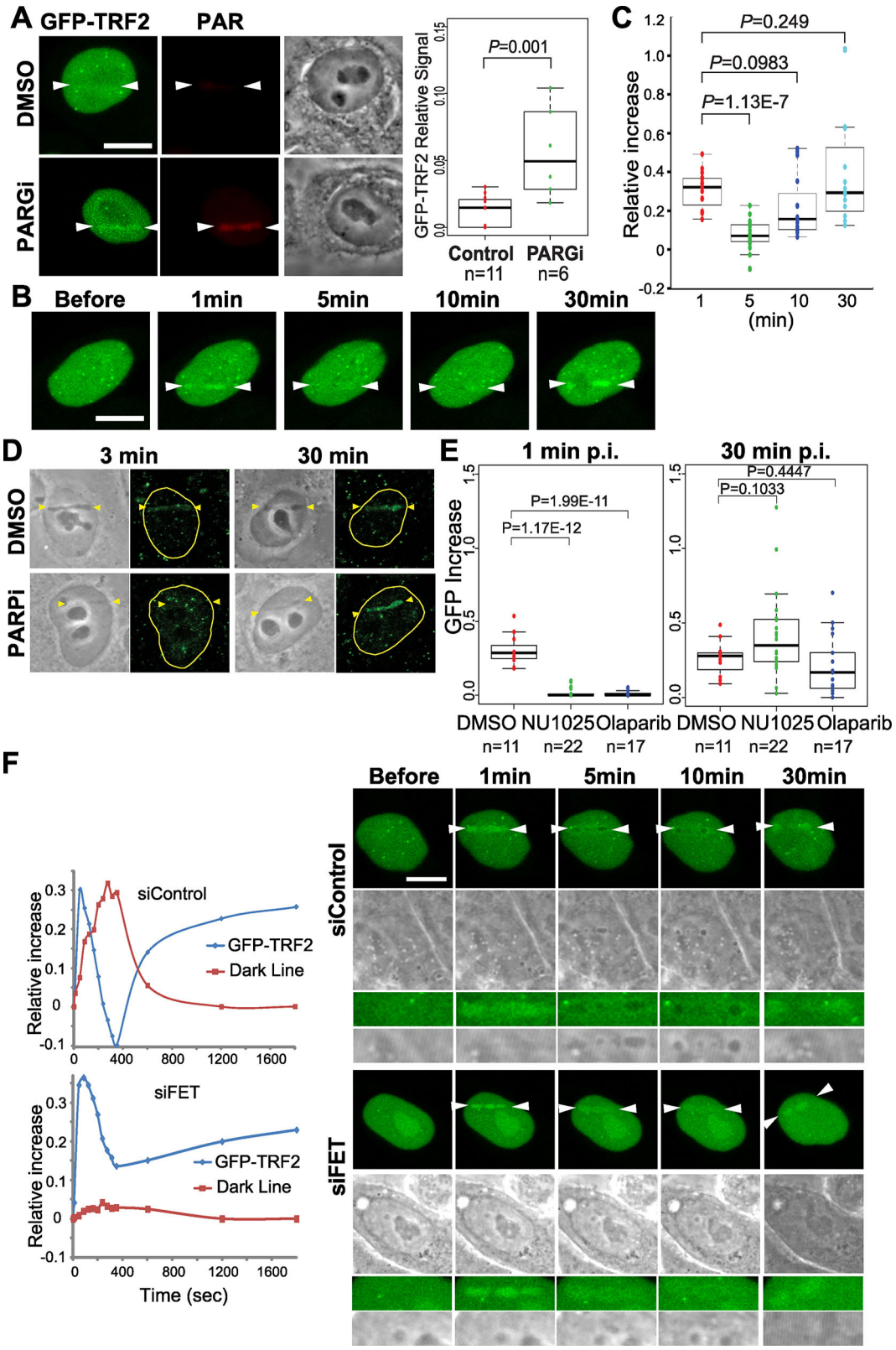

Fig. 1. See next page for legend.

inspection of later time points (20–30 min), however, we found that TRF2 re-appears at damage sites (Fig. 1B,C). Similar recruitment patterns were observed with both the ectopically expressed and endogenous TRF2 (Fig. 1B,D, respectively). The initial recruitment of GFP–TRF2 peaks at ∼1–3 min p.i. (termed 'phase I'), which decreases once but returns peaking at ∼30 min to 1 h ('phase II') (Fig. 1A–C). This phase II recruitment persists for at least 2 h (data not shown). Interestingly, the PARP inhibitors NU1025 and olaparib completely suppressed phase I, but not phase II, recruitment of both endogenous and recombinant TRF2

Journal of Cell Science (2018) 131, jcs219311. doi:10.1242/jcs.219311

Fig. 1. Biphasic TRF2 recruitment to non-telomeric damage sites in nuclei of HeLa cells. (A) PAR stimulation by PARG inhibition (PARGi) promotes GFP–TRF2 accumulation at low input-power damage sites (indicated by arrowheads). Box plot shows quantification of the relative increase of GFP signals at damage sites. (B) Time-course analysis of GFP–TRF2 recruitment to laser-induced DNA damage sites (between arrowheads). (C) Quantification of GFP signals at damage sites in B. *N*=16. (D) Detection of endogenous TRF2 at damage sites. PARP inhibition (PARPi) suppresses phase I, but has no effect on phase II, TRF2 recruitment. (E) Quantification of the effects of PARP inhibitors (NU1025 and olaparib) on immediate (1 min, phase I) and late (30 min, phase II) GFP–TRF2 recruitment. (F) Time course analysis of the effect of IDP depletion on dispersion of TRF2 at damage sites in HeLa cells transfected with control siRNA (siControl) or FET siRNAs (siFET). Left: quantification of signal intensity changes of GFP–TRF2 (blue) and dark line (red). In box plots, the box represents the 25–75th percentiles, and the median is indicated. The whiskers represent the lowest datum still within 1.5× IQR (inter-quartile range) of the lower quartile, and the highest datum still within 1.5× IQR of the upper quartile. Scale bar: 10 µm.

(Fig. 1D,E), suggesting that two phases of TRF2 recruitment are mediated by different mechanisms.

IDPs compete with TRF2 for PARylated DNA lesions

We found that transient GFP–TRF2 displacement is inversely correlated with the appearance of a prominent dark line at damaged lesions readily visible using bright-field microscope imaging (Fig. 1B,F). Close examination at damage sites revealed that GFP signals not only decrease, but are often transiently pushed to the periphery of the damage sites, suggesting that it may be displaced by the constituents of the dark line (Fig. 1B,F). Intrinsically disordered proteins (IDPs) FUS, EWS and TAF15 (collectively, FET), have been shown to accumulate at damage sites in a PAR-dependent manner and are the major components of the dark line (Altmeyer et al., 2015). We found that depletion of FET by siRNA resulted in a more even distribution of the GFP–TRF2 signal at damaged lesions, correlating with disappearance of the dark line (Fig. 1F; Fig. S1A). The results reveal that although both TRF2 and IDPs are recruited to damage sites in a PAR-dependent manner, there is a distinct order of appearance and competition between them, which separates phases I and II.

Phase I and II recruitments are mediated by distinct domains

TRF2 protein domains have been characterized extensively in the context of telomeres. The C-terminal MYB/SANT DNA binding domain of TRF2 specifically recognizes and binds telomere DNA whereas the N-terminal basic domain is not required for telomere targeting (Fig. 2A) (Karlseder et al., 1999; Okamoto et al., 2013). We found that phase I recruitment is abolished by deletion of the N-terminal basic domain, with results similar to those previously reported by Bradshaw et al. (2005) (Fig. 2B,C). In contrast, phase II recruitment was significantly inhibited by deletion of the C-terminal MYB/SANT domain. Deletion of both N- and C-terminal domains abolished both phases of damage site recruitment. Thus, distinct domains play critical roles in rapid and transient phase I and slow and stable phase II. Unlike the previous report (Bradshaw et al., 2005), we found that deletion of the MYB/SANT domain partially reduced phase I recruitment, suggesting that the phase I recruitment is further stabilized by DNA binding of the MYB/SANT domain (Fig. 2C).

Positive charge of the basic domain is required for phase I recruitment

The N-terminal basic domain harbors multiple arginine residues, which may interact with negatively charged PAR residues clustered at damage sites. Indeed, arginine-to-alanine mutations completely abolished the phase I recruitment (Fig. 2D, RA). In contrast, this recruitment is sustained, albeit more weakly, by arginine-to-lysine mutations that preserve the positive charge (Fig. 2D, RK). The basic domain was also shown to bind to the Holliday junction (HJ) (Fouché et al., 2006). However, a HJ binding-defective mutation (H31A) (Poulet et al., 2009) showed no inhibitory effect on TRF2 recruitment to damage sites (Fig. 2D). Thus, the positive charge is essential for the PARP-dependent TRF2 recruitment to non-telomeric DNA damage sites.

TERT contributes to MYB/SANT-dependent phase II recruitment

Human telomerase reverse transcriptase (TERT) is responsible for the addition of telomere sequences. Several studies have indicated that it can also polymerize DNA at non-telomeric DNA ends *de novo* and has a distinct role in DNA damage response (DDR) and repair (Flint et al., 1994; Gao et al., 2008; Majerská et al., 2011; Masutomi et al., 2005; Morin, 1991; Ribeyre and Shore, 2013). Because the MYB/SANT domain, which is responsible for telomere repeat recognition, is pertinent to phase II recruitment, we tested the possible contribution of TERT to TRF2 association at DSB sites. HeLa cells, which express TERT, were treated with siRNA specific for TERT (Fig. 3A; Fig. S2A). We found that the phase II recruitment of TRF2 was partially inhibited by this treatment (Fig. 3A). TRF2, however, can also be recruited to damage sites even in telomerase-negative alternative lengthening of telomeres (ALT) cells, albeit at a lower level (e.g. U2OS cells) (Fig. S2B). Thus, the results indicate that TERT contributes to, but is not essential for, MYB/SANT domain-dependent TRF2 recruitment to damage sites.

Additional domain requirements for phase I and II recruitments

Chimeric mutants combining the domains of TRF1 (also known as TERF1) and TRF2 have provided important insight into the specific role of TRF2 in telomere protection (Okamoto et al., 2013). The N-terminal basic domain is unique to TRF2 (TRF1 has an acidic domain), indicating that phase I recruitment is specific to TRF2. Similarly, we found that the TRF2 TRFH domain required for dimerization (<30% homology with TRF1) is essential for both phase I and II recruitment (Fig. 3B,C; TRFcT). Interestingly, the TRFcH mutant replacing the TRF2 hinge domain with that of TRF1 exhibited intact phase I recruitment, but failed for phase II, indicating that the hinge domain (11% homology to TRF1) is required for phase II recruitment. In contrast, the TRF2 MYB/SANT domain was found to be interchangeable with that for TRF1 for phase II recruitment (both recognize telomere repeats) (Fig. 3B,C; TRFcM).

The hinge domain contains binding sites critical for the interaction between TRF2 and several different factors (Chen et al., 2008; Okamoto et al., 2013). Deletion of the TIN2 binding region (ΔTIN2; amino acids 352–367) critical for TRF2 incorporation into the shelterin complex (Kim et al., 2004; Liu et al., 2004; Ye et al., 2004) had no effect on damage site recruitment, suggesting that TRF2 recruitment to damage sites is independent of the shelterin complex (Fig. 3D). The hinge domain also contains a region critical for suppression of DDR and telomere maintenance, termed 'inhibitor of DDR' (iDDR; amino acids 406–432) (Okamoto et al., 2013). Deletion of this domain (ΔiDDR) recapitulated the phenotype of the TRFcH mutant, inhibiting only the phase II recruitment (Fig. 3D). The iDDR region has previously been shown to be necessary and sufficient for the interaction of TRF2 with the MRE11 complex (Okamoto et al., 2013). We found

Journal of Cell Science (2018) 131, jcs219311. doi:10.1242/jcs.219311

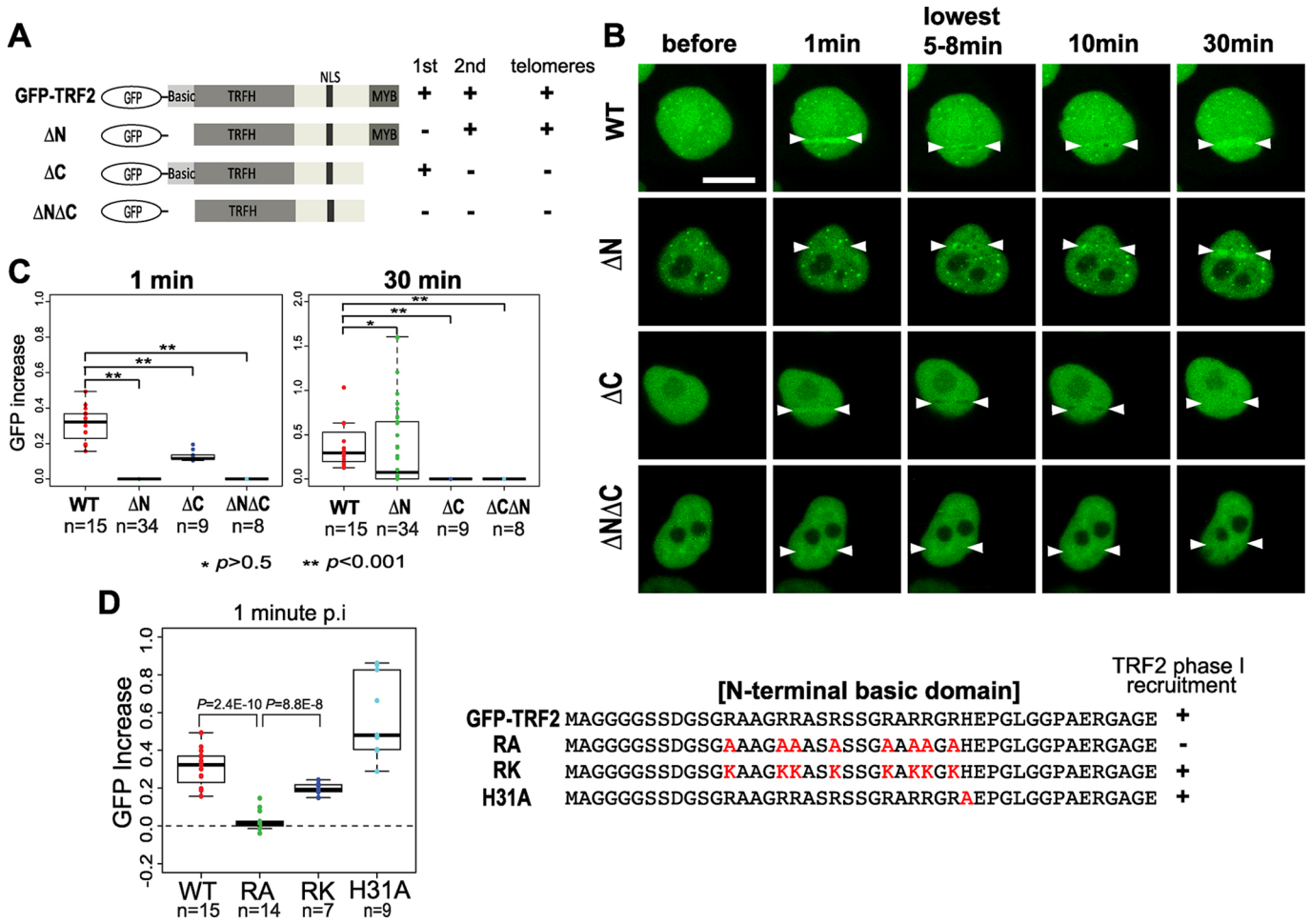

Fig. 2. Distinct TRF2 domain requirement for phase I and II recruitment. (A) Schematic diagrams of TRF2 deletion mutants. (B) Time course analysis of damage site localization (between arrowheads) of wild-type and TRF2 deletion mutants in the nuclei of HeLa cells. (C) Box plot shows quantification of TRF2 mutant GFP signals at damage sites at 1 min (phase I) and 30 min (phase II) post-damage induction. (D) Box plot shows quantification on the effects of the N-terminal amino acid substitutions on phase I recruitment of TRF2. Arginine-to-alanine mutations (RA), arginine-to-lysine substitution (RK) and the HJ binding mutation (H31A) were tested. WT, wild type. Amino acid sequences of N-terminal domain mutations are shown on the right. In box plots, the box represents the 25–75th percentiles, and the median is indicated. The whiskers represent the lowest datum still within 1.5× IQR (inter-quartile range) of the lower quartile, and the highest datum still within 1.5× IQR of the upper quartile. Scale bar: 10 µm.

that siRNA depletion of MRE11 and NBS1 (also known as NBN), the two components of the complex, effectively reduced phase II recruitment (Fig. 3E; Fig. S1B). These results indicate that the MYB/SANT domain-dependent phase II requires the interaction of the iDDR region with the MRE11 complex.

Both phase I and II mechanisms are required for TRF2 accumulation at the I-PpoI-induced DSB sites

I-PpoI endonuclease induces DSB sites in the ribosomal DNA region (Berkovich et al., 2008). Using chromatin immunoprecipitation (ChIP)-qPCR, we found binding of TRF2 to these DSB sites (Fig. 3F). Intriguingly, this binding was further enhanced by methyl methanesulfonate (MMS) treatment, which induces complex damage and stronger PARP activation than simple DSBs. Importantly, TRF2 accumulation at I-PpoI target sites both in the presence and absence of MMS treatment was effectively suppressed by PARP inhibitor, confirming that TRF2 binding to DSB sites is PARP-dependent (Fig. 3F). Interestingly, depletion of the MRE11 complex also abolished TRF2 binding to DSB sites. These results indicate that strong PARP activation is the key determinant for efficient TRF2 recruitment to DSB sites and that both phase I and II recruitment mechanisms are important for the stable binding of TRF2 to DSB sites.

TRF2 facilitates intra-chromosomal HR repair

To determine the significance of TRF2 recruitment to damage sites, the effects of TRF2 depletion were examined using cell-based assays for different pathways of DSB repair (Hu and Parvin, 2014). TRF2 was depleted for 48 h before repair assays in order to minimize telomere erosion, which was typically assayed 4–7 days after depletion (Okamoto et al., 2013; Rai et al., 2016) (Fig. S3). TRF2 has previously been implicated in both HR repair (Mao et al., 2007) and fast repair (suggestive of NHEJ) (Huda et al., 2009). Interestingly, we found that TRF2 depletion reduced the efficiency of HR in the I-SceI-dependent HR assay, but not in the sister chromatid exchange (SCE) assay (Fig. 4A,B). The I-SceI assay selectively captures intra-chromatid or unequal sister chromatid HR, whereas the SCE assay specifically detects sister chromatid conversion (Potts and Yu, 2005). Furthermore, TRF2 depletion had no significant effect on either classical or alternative NHEJ repair (Fig. 4B). Thus, the results indicate that TRF2 plays a specific role in non-sister chromatid HR. Under our

Journal of Cell Science (2018) 131, jcs219311. doi:10.1242/jcs.219311

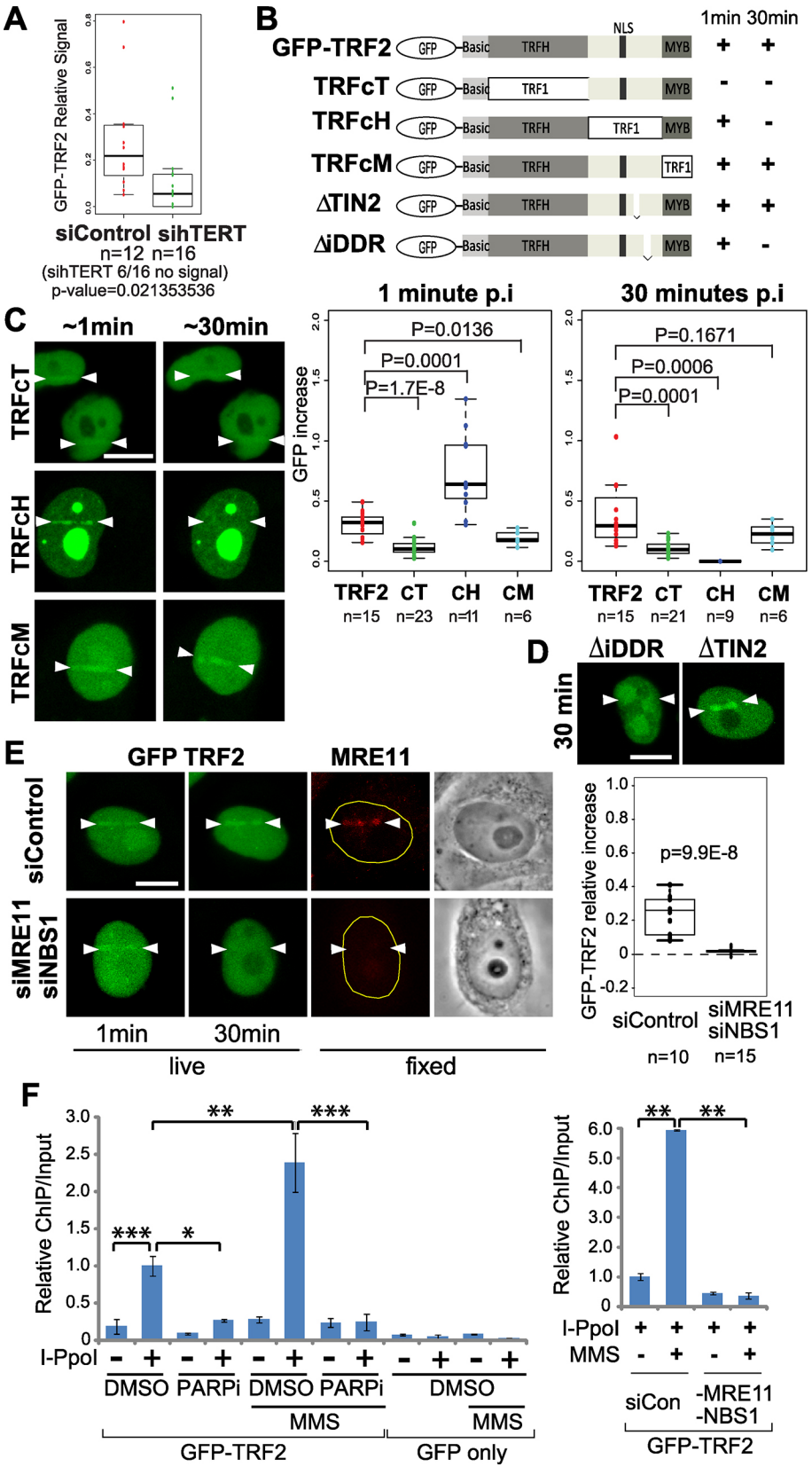

Fig. 3. Phase II recruitment is affected by TERT and is dependent on the iDDR region in the hinge domain of TRF2. (A) Box plot shows that TERT depletion using siRNA inhibits phase II recruitment of TRF2 to DNA damage sites in nuclei of HeLa cells. (B) Schematic diagrams of chimeric TRF1/2 mutants (as previously described in Okamoto et al., 2013) used in the experiments represented in panels C–F. (C) Left: representative cell images of the recruitment of chimeric mutants to damage sites (between arrowheads) at ∼1 min (phase I) and ∼30 min (phase II) after damage induction. Right: box plots show quantification of the GFP–TRF2 signal increase at phase I and phase II at damage sites. (D) Comparison of the GFP signal at damage sites in HeLa cells expressing iDDR and TIN2 deletion mutants at 30 min after damage induction. (E) The effect of MRE11 and NBS1 siRNA (siMRE11 and siNBS1) depletion on phase I and II recruitment of GFP–TRF2 was examined comparing to control siRNA (siControl). HeLa cells were fixed and stained with anti-MRE11 antibody (red) to confirm the depletion. Box plot shows quantification of the GFP–TRF2 signal increase at damage sites in control or MRE11 and NBS1 siRNA-treated cells. (F) ChIP-qPCR analysis of GFP–TRF2 binding at I-PpoI cut sites. TRF2 binding was examined in the absence or presence of I-PpoI, and with and without MMS as indicated. Cells were further treated with DMSO or PARP inhibitor (PARPi) (left panel). Cells expressing GFP only were used as a negative control. Alternatively, cells were transfected with control (siCon) or MRE11 and NBS1 siRNA in the presence of I-PpoI with or without MMS (right panel). In box plots, the box represents the 25–75th percentiles, and the median is indicated. The whiskers represent the lowest datum still within 1.5× IQR (inter-quartile range) of the lower quartile, and the highest datum still within 1.5× IQR of the upper quartile. Bar graphs show mean±s.d., *P<0.01, **P<0.001, ***P<0.0001. Scale bars: 10 µm.

experimental conditions, the effect of TRF2 depletion on I-SceI HR was comparable to that of BRCA1 depletion and can be complemented by expression of wild-type TRF2 (Fig. 4A; Fig. S1C). BRCA1 is a known promoter of HR (Moynahan et al., 1999). Although the N- or C-terminal deletion mutants of TRF2, which primarily affect phase I or phase II, respectively, exhibited variable results, the TRFcT mutant that hinders both phases clearly failed to complement, indicating that both phases are

Journal of Cell Science (2018) 131, jcs219311. doi:10.1242/jcs.219311

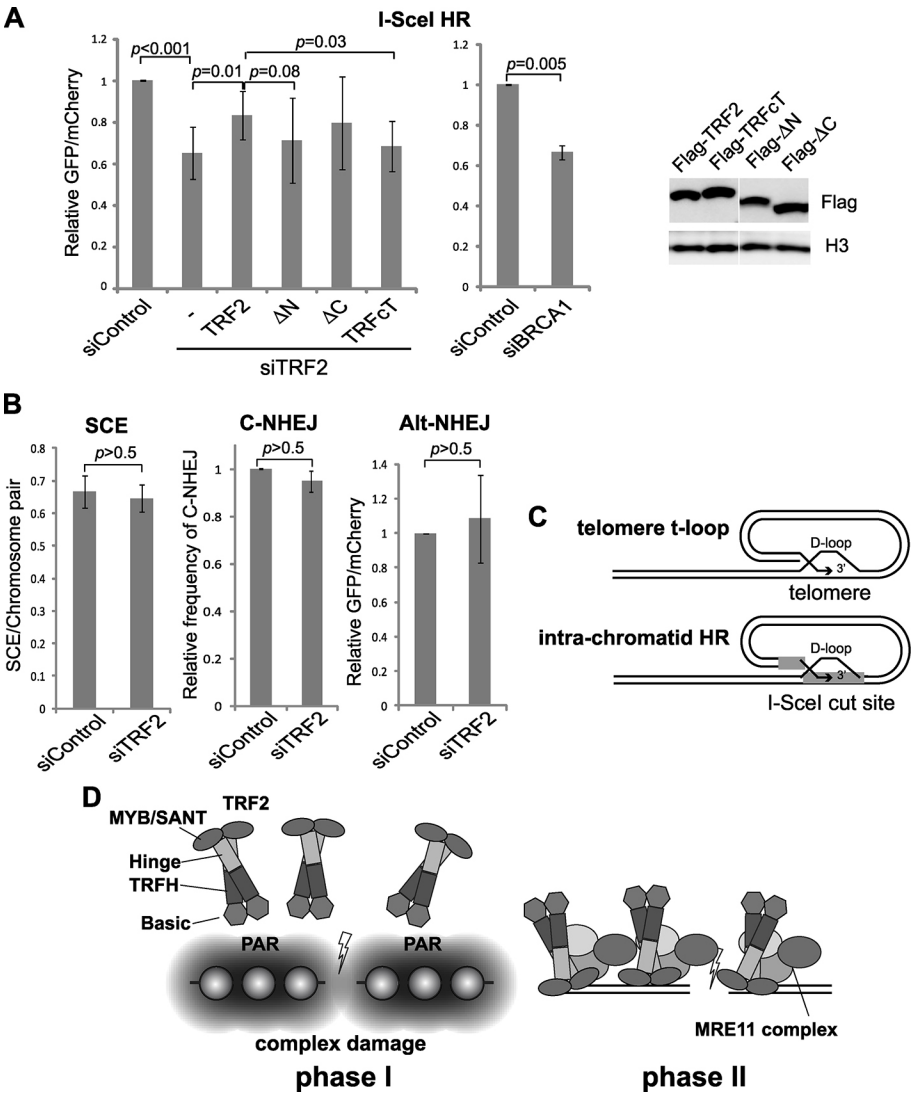

Fig. 4. TRF2 specifically promotes non-sister chromatid HR repair. (A) The effect of TRF2 depletion on DSB repair using the I-SceI HR system. Complementation analysis of TRF2-depleted cells was performed using the wild type and chimeric TRF1/2 mutants. BRCA1 depletion was used as a positive control. Comparable expression levels of the recombinant TRF2 proteins were confirmed using western blot analysis (right). Histone H3 serves as a loading control. (B) The effect of TRF2 depletion on different DSB repair pathways was examined using SCE, classic NHEJ (C-NHEJ) and alternative NHEJ (Alt-NHEJ) assays. (C) Schematic showing similarity between strand invasion in D-loop formation at telomeres and at DSB sites by TRF2. (D) Schematic showing biphasic mechanism of TRF2 recruitment to damage sites. Phase I involves PARP-dependent recruitment through the basic domain. Phase II is mediated by the MYB/SANT domain, which is also dependent on the iDDR region and the Mre11 complex. Bar graphs show mean±s.d.

critical for its optimal repair activity (Fig. 2C, Fig. 3C, Fig. 4). This is consistent with the requirement of both phases for stable TRF2 binding at DSB sites (Fig. 3F).

The selective involvement of TRF2 in non-sister chromatid HR is an interesting contrast to cohesin, which only promotes sister chromatid HR but not other types of HR (Kong et al., 2014; Potts et al., 2006). These differences can be explained by their mechanisms of actions. Cohesin promotes sister chromatid cohesion, therefore promoting pairing of damaged and undamaged sister chromatids for HR. TRF2 promotes loop formation and strand invasion not only at telomere T-loops, but also with non-telomeric templates *in vitro* (Fig. 4C) (Amiard et al., 2007; Doksani et al., 2013; Griffith et al., 1999; Stansel et al., 2001). Furthermore, TRF2 has been shown to inhibit Rad51-mediated D-loop formation with a telomeric, but not non-telomeric, template *in vitro* (Bower and Griffith, 2014). Thus, the cell may hijack the function of TRF2 by clustering the protein to DSB sites to promote intra-chromatid HR, which may be particularly important in the context of complex damage that robustly activates the PARP response.

Our results demonstrate that the initial phase I recruitment by PARP may be critical to bring TRF2 to the proximity of non-telomeric damage sites, which is then further stabilized by the Mre11 complex interaction and DNA binding through the MYB/SANT domain (Fig. 4D). PAR-dependent accumulation of IDPs may compete with phase I recruitment and trigger the second mode of TRF2 association with DNA lesions. Thus, PARP initiates the cascade of dynamic recruitment of factors, some of which compete with each other, to fine-tune repair pathway choice. Interestingly, a recent study showed that BLM is also recruited to damage sites in a biphasic fashion, initially by ATM signaling, and subsequently by the MRE11 complex (Tripathi et al., 2018), suggesting that this type of two-step mechanism may be commonly used to ensure versatility and specificity of factor recruitment.

Conclusion

Our results demonstrate PARP- and MRE11 complex-dependent recruitment of TRF2 to DSB sites, reconciling previous controversies regarding TRF2 recruitment and function at non-telomeric DNA damage sites and revealing a uniquely regulated non-telomeric and shelterin-independent function of TRF2 in non-sister chromatid HR repair.

MATERIALS AND METHODS

Cell lines and synchronization

HeLa and U2OS cells (American Type Culture Collection) were grown in Dulbecco's modified Eagle's medium (DMEM; Gibco) supplemented with

L-glutamine, 10% fetal bovine serum (FBS) and antibiotics. HeLa DR–GFP (for HR assay) (Hu and Parvin, 2014; Pierce et al., 2001) and EJ2–GFP (for alternative NHEJ assay) (Bennardo et al., 2008) stable cells were grown in DMEM with high glucose (4500 mg/l), supplemented with 10% (v/v) FBS (Omega Scientific), 1% pen/strep, 1% GlutaMAX (both Gibco) and 1.5 µg/ml puromycin (Sigma). 293/HW1 cells (for classic NHEJ assay) (Zhuang et al., 2009) were grown in DMEM (high glucose), 1% pen/strep, 1% sodium pyruvate, 1% GlutaMAX (all Gibco), 10% FBS (Omega Scientific), and 2 µg/ml puromycin (Sigma). All the cell lines were mycoplasma-negative.

TRF2 mutants

The expression plasmids containing GFP–TRF2 full-length, deletion or TRF1/2 chimeric mutants were kindly provided by Dr Eros Lazzerini Denchi (The Scripps Research Institute, La Jolla, CA, USA) (Okamoto et al., 2013). These cDNAs were also re-cloned into a pIRES vector containing an N-terminal FLAG epitope. Those include TRF2ΔN (amino acids 45–500), TRF2ΔC (amino acids 1–454), TRF2ΔNΔC (amino acids 45–454), ΔTIN2, and TRFcT (Okamoto et al., 2013). RA and RK mutants were as described previously (Mitchell et al., 2009).

Antibodies

Mouse monoclonal antibodies specific for PAR polymers [BML-SA216–0100, Enzo Life Sciences; 1:500 dilution for immunofluorescence staining (IF)], TRF2 (NB100–56506, Novus Biologicals; 1:500 for IF), MRE11 [GTX70212, GeneTex; 1:500 for IF, 1:1000 for western blotting (WB)], GFP (632592, Takara Bio; 1:500 for ChIP), Actin (A4700, Sigma; 1:1000 for WB), FLAG (F3165, Sigma; 1:1000 for WB), and BRCA1 (GTX70111, GeneTex; 1:1000 for WB), as well as rabbit polyclonal antibodies specific for γH2AX (GTX628789, GeneTex; 1:500 for IF), EWSR1 (GTX114069, GeneTex; 1:1000 for WB), TAF15 (GTX103116, GeneTex; 1:1000 for WB), H3 (14-411, Upstate Bio; 1:1000 for WB) and Rad21 (Kong et al., 2014; 1:2000 for WB) were used.

Immunofluorescence staining

At different time points after damage induction, cells were fixed in 4% paraformaldehyde (15 min at 4°C), permeabilized in 0.5% Triton X-100 for 5 min (4°C), and stained with antibodies. The staining procedure was as described previously (Kim et al., 2002). Fluorescence images were captured through a 100× Ph3 UPlanFI oil objective lens (NA, 1.3; Olympus) on a model IX81 Olympus microscope with a charge-coupled device camera.

Western blotting

Protein samples were subjected to SDS-PAGE and then transferred to nitrocellulose membranes as described previously (Schmiesing et al., 1998). The membranes were blocked with Pierce Protein-Free T20 (PBS) Blocking Buffer (Thermo Fisher Scientific). The primary antibody was incubated in 3% BSA+0.05% Tween 20 in PBS for 1 h at room temperature or overnight at 4C°, followed by three washes in PBS+0.05% Tween 20. The secondary antibody conjugated to HRP (anti-mouse-IgG, W4021; anti-rabbit-IgGm W4011, both used at 1:10,000; Promega) was incubated in 3% BSA+0.05% Tween 20 in PBS for 1 h at room temperature. The filter was then washed three times in PBS+0.05% Tween 20 and developed with SuperSignal West Pico Chemiluminescent Substrate (Thermo Fisher Scientific). Images were acquired using the Image Analyzer (LAS-4000, Fujifilm) and analyzed using Quantity One software (Bio-Rad).

Laser damage induction and cell imaging

Near-infrared (NIR) femtosecond laser irradiation was carried out using a Zeiss LSM 510 META multiphoton-equipped (3.0 W 170 fs coherent tunable Chameleon Ultra-NIR laser) confocal microscope. The Chameleon Ultra-NIR beam was tuned to 780 nm, where the software bleach function was used to target linear tracts inside the cell nuclei for exposure to single laser scans (12.8 µs pixel dwell time) through the 100× objective lens (1.3 NA Zeiss Plan APO) (Cruz et al., 2015). The peak irradiance at the focal point for the higher input laser power is 5.27×10^{10} W/cm^2, and for the lower input laser power is 3.24×10^{10} W/cm^2 (Cruz et al., 2015). Fluorescence measurement of the recruitment of GFP–TRF2 wild type and mutant proteins, and other GFP-tagged proteins, to damage sites was analyzed using live-cell confocal scanning with the 488 nm CW argon laser on the Zeiss LSM 510 META platform. The signals were measured with the LSM 510 software (version 4.0). The data were collected in three separate experiments. *P*-values were calculated by two-tailed *t*-test using Excel software (Microsoft). Boxplots were created with R program (https://www.r-project.org).

siRNA depletion

HeLa cells were transfected twice, 24 h apart, with siRNAs at a final concentration of 5 nM using HiPerFect (Qiagen) transfection reagent according to the manufacturer's instructions. siRNAs directed against TERT (5′-TTTCATCAGCAAGTTTGGA-3′; Masutomi et al., 2005), MRE11 (5′-GCTAATGACTCTGATGATA-3′; Myers and Cortez, 2006), NBS1 (5′-GAAGAAACGTGAACTCAAG-3′; Myers and Cortez, 2006), human TRF2 (SI00742630, Qiagen), BRCA1 (5′-GCTCCTCTCACTCTTCAGT-3′; Hu and Parvin, 2014), FET [FUS (s5402), EWSR1 (s4886) and TAF15 (s15656); Ambion/LifeTechnologies; Altmeyer et al., 2015], and a negative-control siRNA (1027310, Qiagen) were used. Cells were harvested for western blot analyses or were subjected to laser micro-irradiation, approximately 48 h after the final transfection.

Inhibitor treatment

20 µM PARP inhibitor olaparib (Apexbio Technology) or 1 µM PARG inhibitor (PARGi) 6,9-diamino-2-ethoxyacridine lactate monohydrate (DEA; Trevigen) was added to the cell culture 1 h prior to damage induction. DMSO only was added to control cells.

DSB induction using I-PpoI endonuclease and ChIP-qPCR analysis

The experimental procedure was previously described (Kong et al., 2014). Briefly, HeLa cells were transfected with expression plasmids encoding GFP–TRF2 (or GFP only) with or without ER-I-PpoI expression plasmid. 24 h later, 4-hydroxy-tamoxifen (4-OHT; Sigma) was added to a final concentration of 1 µM for 10 h to induce DNA damage. For MMS-treated cells, 3 mM MMS was added 1 h before harvest. DMSO or PARP inhibitor was added 1 h before MMS treatment. For the MRE11 and NBS1 depletion experiment, two rounds of control or MRE11 siRNA and NBS1 siRNA transfection were performed 48 h and 24 h before GFP–TRF2 and/or ER-I-PpoI plasmid transfection. ChIP analysis was performed, using GFP antibody, as described previously (Berkovich et al., 2008; Kong et al., 2014). The data represent the means±s.d. of two separate experiments. Four samples (absence or presence of I-PpoI, and with and without MMS) were repeated the third time, and results with the same trend were obtained. *P*-values were calculated by two-tailed *t*-test.

DSB repair assays

Homologous recombination (HR) and alternative NHEJ assays were performed as described previously in HeLa cells (Bennardo et al., 2008; Hu and Parvin, 2014) with modification. Briefly, on day 1, the appropriate cell lines [stable cell lines expressing appropriate repair templates; HeLa DR–GFP for the HR assay (Hu and Parvin, 2014; Pierce et al., 2001); EJ2–GFP for the alternative NHEJ assay (Bennardo et al., 2008), and 293/HW1 for the classic NHEJ assay (Zhuang et al., 2009)] were seeded in 24-well plates. The next day, cells at 50% confluence were transfected with TRF2 siRNA or control siRNA. On day 3, cells were re-transfected with the same siRNA for 5–6 h, and then were transferred to 35 mm wells. On day 4, the plasmid encoding I-SceI endonuclease was co-transfected with mCherry-expressing plasmid to induce DSBs. The cells were examined using flow cytometry on day 7, and the ratio of the GFP reporter to mCherry was used as a measure of HR or alternative NHEJ efficiency. The classic NHEJ assay utilizes real-time qPCR and was carried out as described (Hu and Parvin, 2014; Zhuang et al., 2009) in 293 cells with modification. The transfection procedure was as described above. For plasmid add-back in the rescue assays, the transfection procedure was the same except that at the second siRNA transfection, the blank control plasmid, and plasmids encoding FLAG–TRF2 and corresponding mutants were co-transfected into the cells using Lipofectamine 3000 (Thermo Fisher Scientific). The data represent the means±s.d. of three separate experiments. *P*-values were calculated by two-tailed *t*-test.

Acknowledgements
We thank Dr Jeff Parvin (Department of Biomedical Informatics, The Ohio State University, Columbus, OH) for kindly providing DSB repair assay cell lines, Dr Eros Lazzerini Denchi (The Scripps Research Institute, La Jolla, CA) for TRF mutant plasmids, and Dr Feng Qiao (Department of Biological Chemistry, School of Medicine, University of California, Irvine, CA) for helpful discussion and advice.

Competing interests
The authors declare no competing or financial interests.

Author contributions
Conceptualization: X.K., K.Y.; Methodology: X.K., G.M.S.C., M.W.B., K.Y.; Validation: X.K., G.M.S.C., K.Y.; Formal analysis: X.K., M.W.B., K.Y.; Investigation: X.K., S.L.T., K.Y.; Resources: X.K., X.-D.Z., K.Y.; Data curation: X.K., G.M.S.C., K.Y.; Writing - original draft: X.K., K.Y.; Writing - review & editing: X.K., G.M.S.C., S.L.T., X.-D.Z., M.W.B., K.Y.; Visualization: X.K., G.M.S.C., K.Y.; Supervision: X.K., M.W.B., K.Y.; Project administration: K.Y.; Funding acquisition: M.W.B., K.Y.

Funding
This work was supported by the National Science Foundation [grant MCB-1615701 to K.Y.] and the Air Force Office of Scientific Research [grant FA9550-08-1-0384], and gifts from the Beckman Laser Institute and Medical Clinic, the Hoag Family Foundation, and the David and Lucile Packard Foundation (M.W.B.), and by the Canadian Institutes of Health Research [grant MOP-86620 to X.-D.Z.].

Supplementary information
Supplementary information available online at
http://jcs.biologists.org/lookup/doi/10.1242/jcs.219311.supplemental

References

Ahel, D., Horejsí, Z., Wiechens, N., Polo, S. E., Garcia-Wilson, E., Ahel, I., Flynn, H., Skehel, M., West, S. C., Jackson, S. P. et al. (2009). Poly(ADP-ribose)-dependent regulation of DNA repair by the chromatin remodeling enzyme ALC1. *Science* **325**, 1240-1243.

Altmeyer, M., Neelsen, K. J., Teloni, F., Pozdnyakova, I., Pellegrino, S., Grøfte, M., Rask, M.-B. D., Streicher, W., Jungmichel, S., Nielsen, M. L. et al. (2015). Liquid demixing of intrinsically disordered proteins is seeded by poly(ADP-ribose). *Nat. Commun.* **6**, 8088.

Amiard, S., Doudeau, M., Pinte, S., Poulet, A., Lenain, C., Faivre-Moskalenko, C., Angelov, D., Hug, N., Vindigni, A., Bouvet, P. et al. (2007). A topological mechanism for TRF2-enhanced strand invasion. *Nat. Struc. Mol. Biol.* **14**, 147-154.

Ayrapetov, M. K., Gursoy-Yuzugullu, O., Xu, C., Xu, Y. and Price, B. D. (2014). DNA double-strand breaks promote methylation of histone H3 on lysine 9 and transient formation of repressive chromatin. *Proc. Natl. Acad. Sci. USA* **111**, 9169-9174.

Ball, A. R., Jr. and Yokomori, K. (2011). Damage site chromatin: open or closed? *Curr. Opin. Cell Biol.* **23**, 277-283.

Beck, C., Robert, I., Reina-San-Martin, B., Schreiber, V. and Dantzer, F. (2014). Poly(ADP-ribose) polymerases in double-strand break repair: focus on PARP1, PARP2 and PARP3. *Exp. Cell Res.* **329**, 18-25.

Bennardo, N., Cheng, A., Huang, N. and Stark, J. M. (2008). Alternative-NHEJ is a mechanistically distinct pathway of mammalian chromosome break repair. *PLoS Genet.* **4**, e1000110.

Berkovich, E., Monnat, R. J., Jr. and Kastan, M. B. (2008). Assessment of protein dynamics and DNA repair following generation of DNA double-strand breaks at defined genomic sites. *Nat. Protoc.* **3**, 915-922.

Bilaud, T., Brun, C., Ancelin, K., Koering, C. E., Laroche, T. and Gilson, E. (1997). Telomeric localization of TRF2, a novel human telobox protein. *Nat. Genet.* **17**, 236-239.

Bower, B. D. and Griffith, J. D. (2014). TRF1 and TRF2 differentially modulate Rad51-mediated telomeric and nontelomeric displacement loop formation in vitro. *Biochemistry* **53**, 5485-5495.

Bradshaw, P. S., Stavropoulos, D. J. and Meyn, M. S. (2005). Human telomeric protein TRF2 associates with genomic double-strand breaks as an early response to DNA damage. *Nat. Genet.* **37**, 193-197.

Chen, Y., Yang, Y., van Overbeek, M., Donigian, J. R., Baciu, P., de Lange, T. and Lei, M. (2008). A shared docking motif in TRF1 and TRF2 used for differential recruitment of telomeric proteins. *Science* **319**, 1092-1096.

Chou, D. M., Adamson, B., Dephoure, N. E., Tan, X., Nottke, A. C., Hurov, K. E., Gygi, S. P., Colaiácovo, M. P. and Elledge, S. J. (2010). A chromatin localization screen reveals poly (ADP ribose)-regulated recruitment of the repressive polycomb and NuRD complexes to sites of DNA damage. *Proc. Natl. Acad. Sci. USA* **107**, 18475-18480.

Cruz, G. M. S., Kong, X., Silva, B. A., Khatibzadeh, N., Thai, R., Berns, M. W. and Yokomori, K. (2015). Femtosecond near-infrared laser microirradiation reveals a crucial role for PARP signaling on factor assemblies at DNA damage sites. *Nucleic Acids Res.* **44**, e27.

Daniels, C. M., Ong, S.-E. and Leung, A. K. L. (2015). The promise of proteomics for the study of ADP-ribosylation. *Mol. Cell* **58**, 911-924.

de Lange, T. (2002). Protection of mammalian telomeres. *Oncogene* **21**, 532-540.

Doksani, Y., Wu, J. Y., de Lange, T. and Zhuang, X. (2013). Super-resolution fluorescence imaging of telomeres reveals TRF2-dependent T-loop formation. *Cell* **155**, 345-356.

Feuerhahn, S., Chen, L.-Y., Luke, B. and Porro, A. (2015). No DDRama at chromosome ends: TRF2 takes centre stage. *Trends Biochem. Sci.* **40**, 275-285.

Flint, J., Craddock, C. F., Villegas, A., Bentley, D. P., Williams, H. J., Galanello, R., Cao, A., Wood, W. G., Ayyub, H. and Higgs, D. R. (1994). Healing of broken human chromosomes by the addition of telomeric repeats. *Am. J. Hum. Genet.* **55**, 505-512.

Fouché, N., Cesare, A. J., Willcox, S., Özgür, S., Compton, S. A. and Griffith, J. D. (2006). The basic domain of TRF2 directs binding to DNA junctions irrespective of the presence of TTAGGG repeats. *J. Biol. Chem.* **281**, 37486-37495.

Gao, Q., Reynolds, G. E., Wilcox, A., Miller, D., Cheung, P., Artandi, S. E. and Murnane, J. P. (2008). Telomerase-dependent and -independent chromosome healing in mouse embryonic stem cells. *DNA Repair* **7**, 1233-1249.

Gottschalk, A. J., Timinszky, G., Kong, S. E., Jin, J., Cai, Y., Swanson, S. K., Washburn, M. P., Florens, L., Ladurner, A. G., Conaway, J. W. et al. (2009). Poly(ADP-ribosyl)ation directs recruitment and activation of an ATP-dependent chromatin remodeler. *Proc. Natl. Acad. Sci. USA* **106**, 13770-13774.

Griffith, J. D., Comeau, L., Rosenfield, S., Stansel, R. M., Bianchi, A., Moss, H. and de Lange, T. (1999). Mammalian telomeres end in a large duplex loop. *Cell* **97**, 503-514.

Hu, Y. and Parvin, J. D. (2014). Small ubiquitin-like modifier (SUMO) isoforms and conjugation-independent function in DNA double-strand break repair pathways. *J. Biol. Chem.* **289**, 21289-21295.

Huda, N., Tanaka, H., Mendonca, M. S. and Gilley, D. (2009). DNA damage-induced phosphorylation of TRF2 is required for the fast pathway of DNA double-strand break repair. *Mol. Cell. Biol.* **29**, 3597-3604.

Huda, N., Abe, S., Gu, L., Mendonca, M. S., Mohanty, S. and Gilley, D. (2012). Recruitment of TRF2 to laser-induced DNA damage sites. *Free Radic. Biol. Med.* **53**, 1192-1197.

Izhar, L., Adamson, B., Ciccia, A., Lewis, J., Pontano-Vaites, L., Leng, Y., Liang, A. C., Westbrook, T. F., Harper, J. W. and Elledge, S. J. (2015). A systematic analysis of factors localized to damaged chromatin reveals PARP-dependent recruitment of transcription factors. *Cell Rep.* **11**, 1486-1500.

Kalisch, T., Amé, J.-C., Dantzer, F. and Schreiber, V. (2012). New readers and interpretations of poly(ADP-ribosyl)ation. *Trends Biochem. Sci.* **37**, 381-390.

Karlseder, J., Broccoli, D., Dai, Y., Hardy, S. and de Lange, T. (1999). p53- and ATM-dependent apoptosis induced by telomeres lacking TRF2. *Science* **283**, 1321-1325.

Karlseder, J., Hoke, K., Mirzoeva, O. K., Bakkenist, C., Kastan, M. B., Petrini, J. H. J. and de Lange, T. (2004). The telomeric protein TRF2 binds the ATM kinase and can inhibit the ATM-dependent DNA damage response. *PLoS Biol.* **2**, e240.

Khoury-Haddad, H., Guttmann-Raviv, N., Ipenberg, I., Huggins, D., Jeyasekharan, A. D. and Ayoub, N. (2014). PARP1-dependent recruitment of KDM4D histone demethylase to DNA damage sites promotes double-strand break repair. *Proc. Natl. Acad. Sci. USA* **111**, E728-E737.

Kim, J.-S., Krasieva, T. B., LaMorte, V. J., Taylor, A. M. R. and Yokomori, K. (2002). Specific recruitment of human cohesin to laser-induced DNA damage. *J. Biol. Chem.* **277**, 45149-45153.

Kim, S.-H., Beausejour, C., Davalos, A. R., Kaminker, P., Heo, S.-J. and Campisi, J. (2004). TIN2 mediates functions of TRF2 at human telomeres. *J. Biol. Chem.* **279**, 43799-43804.

Kong, X., Stephens, J., Ball, A. R., Jr, Heale, J. T., Newkirk, D. A., Berns, M. W. and Yokomori, K. (2011). Condensin I recruitment to base damage-enriched DNA lesions is modulated by PARP1. *PLoS ONE* **6**, e23548.

Kong, X., Ball, A. R., Jr, Pham, H. X., Zeng, W., Chen, H.-Y., Schmiesing, J. A., Kim, J.-S., Berns, M. and Yokomori, K. (2014). Distinct functions of human cohesin-SA1 and cohesin-SA2 in double-strand break repair. *Mol. Cell. Biol.* **34**, 685-698.

Larsen, D. H., Poinsignon, C., Gudjonsson, T., Dinant, C., Payne, M. R., Hari, F. J., Rendtlew Danielsen, J. M., Menard, P., Sand, J. C., Stucki, M. et al. (2010). The chromatin-remodeling factor CHD4 coordinates signaling and repair after DNA damage. *J. Cell Biol.* **190**, 731-740.

Liu, D., O'Connor, M. S., Qin, J. and Songyang, Z. (2004). Telosome, a mammalian telomere-associated complex formed by multiple telomeric proteins. *J. Biol. Chem.* **279**, 51338-51342.

Majerská, J., Sýkorová, E. and Fajkus, J. (2011). Non-telomeric activities of telomerase. *Mol. Biosyst.* **7**, 1013-1023.

Mao, Z., Seluanov, A., Jiang, Y. and Gorbunova, V. (2007). TRF2 is required for repair of nontelomeric DNA double-strand breaks by homologous recombination. *Proc. Natl. Acad. Sci. USA* **104**, 13068-13073.

Masutomi, K., Possemato, R., Wong, J. M. Y., Currier, J. L., Tothova, Z., Manola, J. B., Ganesan, S., Lansdorp, P. M., Collins, K. and Hahn, W. C. (2005). The telomerase reverse transcriptase regulates chromatin state and DNA damage responses. *Proc. Natl. Acad. Sci. USA* **102**, 8222-8227.

Mitchell, T. R. H., Glenfield, K., Jeyanthan, K. and Zhu, X.-D. (2009). Arginine methylation regulates telomere length and stability. *Mol. Cell. Biol.* **29**, 4918-4934.

Morin, G. B. (1991). Recognition of a chromosome truncation site associated with alpha-thalassaemia by human telomerase. *Nature* **353**, 454-456.

Moynahan, M. E., Chiu, J. W., Koller, B. H. and Jasin, M. (1999). Brca1 controls homology-directed DNA repair. *Mol. Cell* **4**, 511-518.

Myers, J. S. and Cortez, D. (2006). Rapid activation of ATR by ionizing radiation requires ATM and Mre11. *J. Biol. Chem.* **281**, 9346-9350.

Okamoto, K., Bartocci, C., Ouzounov, I., Diedrich, J. K., Yates, J. R., III and Denchi, E. L. (2013). A two-step mechanism for TRF2-mediated chromosome-end protection. *Nature* **494**, 502-505.

Pierce, A. J., Hu, P., Han, M., Ellis, N. and Jasin, M. (2001). Ku DNA end-binding protein modulates homologous repair of double-strand breaks in mammalian cells. *Genes Dev.* **15**, 3237-3242.

Polo, S. E., Kaidi, A., Baskcomb, L., Galanty, Y. and Jackson, S. P. (2010). Regulation of DNA-damage responses and cell-cycle progression by the chromatin remodelling factor CHD4. *EMBO J.* **29**, 3130-3139.

Potts, P. R. and Yu, H. (2005). Human MMS21/NSE2 is a SUMO ligase required for DNA repair. *Mol. Cell. Biol.* **25**, 7021-7032.

Potts, P. R., Porteus, M. H. and Yu, H. (2006). Human SMC5/6 complex promotes sister chromatid homologous recombination by recruiting the SMC1/3 cohesin complex to double-strand breaks. *EMBO J.* **25**, 3377-3388.

Poulet, A., Buisson, R., Faivre-Moskalenko, C., Koelblen, M., Amiard, S., Montel, F., Cuesta-Lopez, S., Bornet, O., Guerlesquin, F., Godet, T. et al. (2009). TRF2 promotes, remodels and protects telomeric Holliday junctions. *EMBO J.* **28**, 641-651.

Rai, R., Chen, Y., Lei, M. and Chang, S. (2016). TRF2-RAP1 is required to protect telomeres from engaging in homologous recombination-mediated deletions and fusions. *Nat. Commun.* **7**, 10881.

Ribeyre, C. and Shore, D. (2013). Regulation of telomere addition at DNA double-strand breaks. *Chromosoma* **122**, 159-173.

Schmiesing, J. A., Ball, A. R., Gregson, H. C., Alderton, J. M., Zhou, S. and Yokomori, K. (1998). Identification of two distinct human SMC protein complexes involved in mitotic chromosome dynamics. *Proc. Natl. Acad. Sci. USA* **95**, 12906-12911.

Smeenk, G., Wiegant, W. W., Vrolijk, H., Solari, A. P., Pastink, A. and van Attikum, H. (2010). The NuRD chromatin-remodeling complex regulates signaling and repair of DNA damage. *J. Cell Biol.* **190**, 741-749.

Stansel, R. M., de Lange, T. and Griffith, J. D. (2001). T-loop assembly in vitro involves binding of TRF2 near the 3' telomeric overhang. *EMBO J.* **20**, 5532-5540.

Sun, Y., Jiang, X., Xu, Y., Ayrapetov, M. K., Moreau, L. A., Whetstine, J. R. and Price, B. D. (2009). Histone H3 methylation links DNA damage detection to activation of the tumour suppressor Tip60. *Nat. Cell Biol.* **11**, 1376-1382.

Tripathi, V., Agarwal, H., Priya, S., Batra, H., Modi, P., Pandey, M., Saha, D., Raghavan, S. C. and Sengupta, S. (2018). MRN complex-dependent recruitment of ubiquitylated BLM helicase to DSBs negatively regulates DNA repair pathways. *Nat. Commun.* **9**, 1016.

van Steensel, B., Smogorzewska, A. and de Lange, T. (1998). TRF2 protects human telomeres from end-to-end fusions. *Cell* **92**, 401-413.

Williams, E. S., Stap, J., Essers, J., Ponnaiya, B., Luijsterburg, M. S., Krawczyk, P. M., Ullrich, R. L., Aten, J. A. and Bailey, S. M. (2007). DNA double-strand breaks are not sufficient to initiate recruitment of TRF2. *Nat. Genet.* **39**, 696-698.

Ye, J. Z.-S., Donigian, J. R., van Overbeek, M., Loayza, D., Luo, Y., Krutchinsky, A. N., Chait, B. T. and de Lange, T. (2004). TIN2 binds TRF1 and TRF2 simultaneously and stabilizes the TRF2 complex on telomeres. *J. Biol. Chem.* **279**, 47264-47271.

Zhuang, J., Jiang, G., Willers, H. and Xia, F. (2009). Exonuclease function of human Mre11 promotes deletional nonhomologous end joining. *J. Biol. Chem.* **284**, 30565-30573.

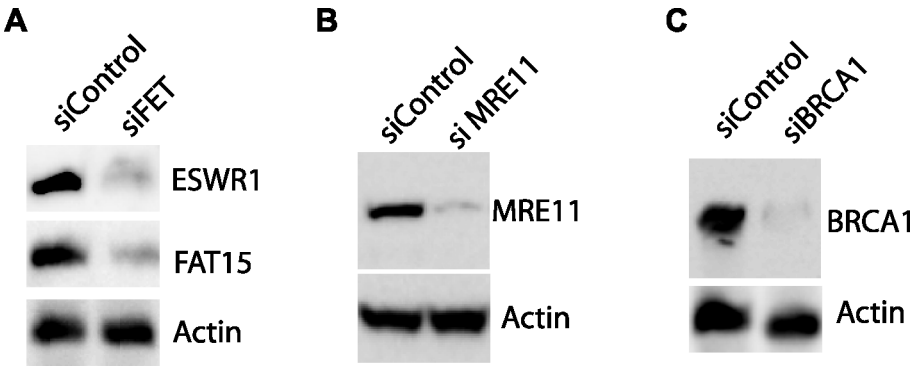

Figure S1

Co-depletion of ESWR1 and FET by siRNA specific for FET is confirmed by western blot (**A**). Actin serves as a loading control. Similarly, depletion of Mre11 (**B**) and BRCA1 (**C**) by corresponding siRNAs were confirmed.

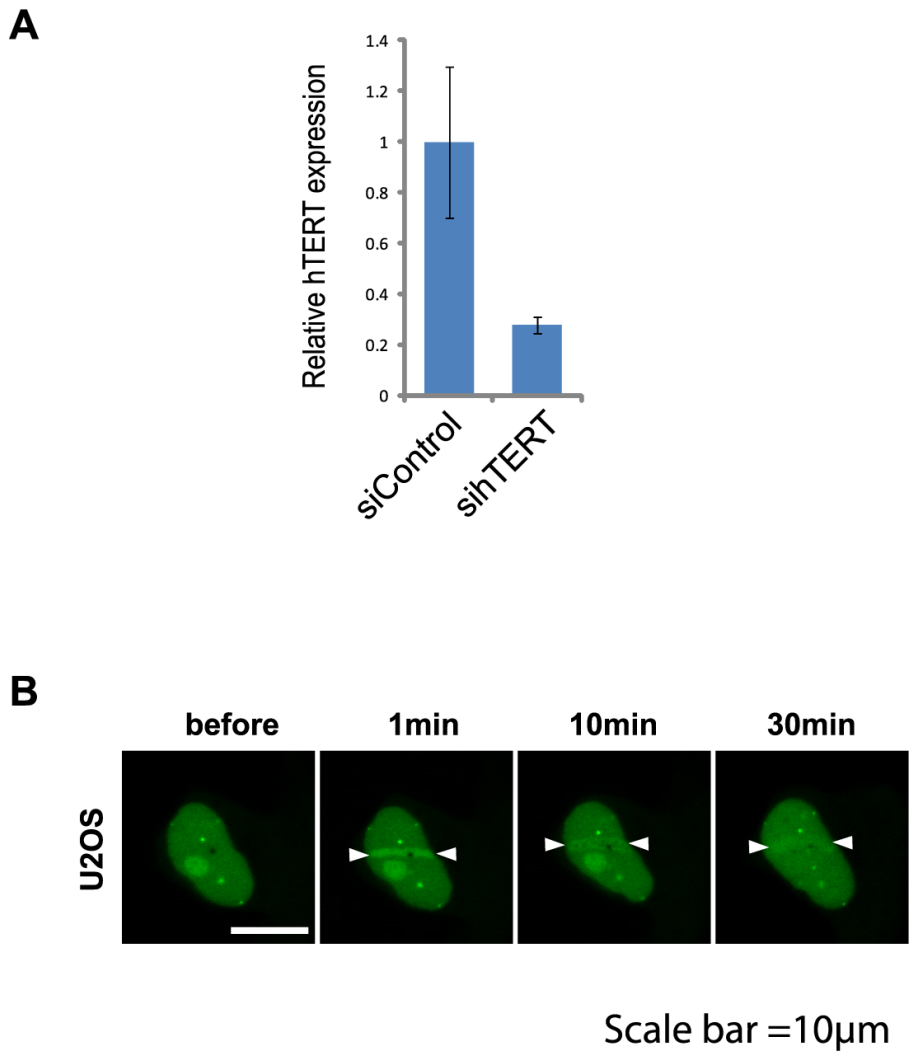

Figure S2

A. RT qPCR analysis of hTERT depletion in HeLa cells. The mRNA level of hTERT was normalized to GAPDH. hTERT qPCR primers used are 5'-CGGAAGAGTGTCTGGAGCAA-3' (forward) and 5'-GGATGAAGCGGAGTCTGGA-3'(reverse) (Liu et al., 2013).

B. An example of the time course analysis of GFP-TRF2 recruitment to the laser-induced damage sites in U2OS cells. Scale bar=10μm.

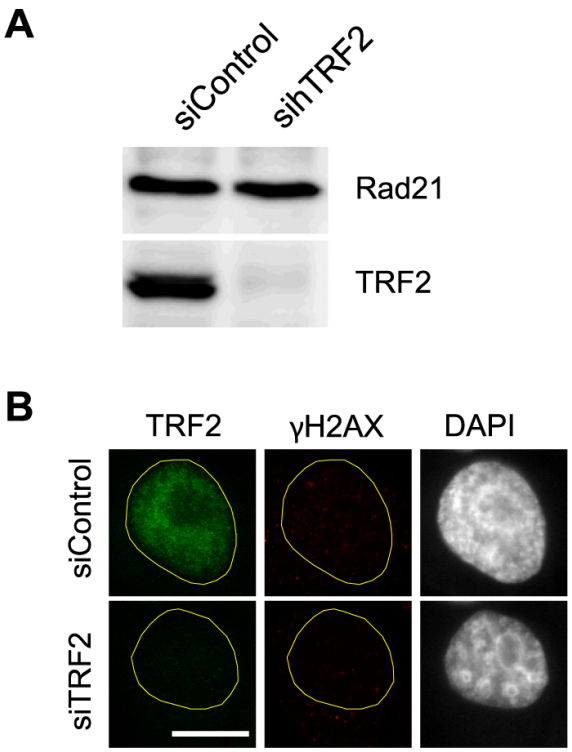

Figure S3

A. Analysis of TRF2 depletion in HeLa cells after siRNA transfection by Western blot. Total cell lysates from control or TRF2 siRNA-transfected cells were subjected to western blot analysis using anti-TRF2 antibody. Rad21 was used as a loading control.

B. Telomere dysfunction-induced foci (TIF) analysis. Cells were treated with control or TRF2 siRNA and were fixed at 48hrs after 2nd siRNA transfection. Cells were stained with antibodies specific for TRF2 and γH2AX, and DAPI as indicated at the top. TRF2 depleted cells didn't show any increase of γH2AX foci indicative of TIF.